J Mater Sci (2012) 47:3383–3390
DOI 10.1007/s10853-011-6183-3

Branched chain polymeric metal complexes containing Co(II) or Ni(II) complexes with a donor–π–acceptor architecture: synthesis, characterization, and photovoltaic applications

Jinyan Deng · Qian Xiu · Lihui Guo · Lirong Zhang · Gaojun Wen · Chaofan Zhong

Received: 16 October 2011 / Accepted: 5 December 2011 / Published online: 17 December 2011

Abstract Four donor–π–acceptor type polymeric metal complexes (PCo–F, PCo–B, PNi–F, and PNi–B) with Co(II) or Ni(II) complexes in the branched chain were synthesized by the Heck coupling and utilized as dyes for dye-sensitized solar cells (DSSCs). The structures, photophysical, electrochemicals, and thermal properties of the four dyes were investigated in detail, and the results showed that dye containing Ni(II) complex and alkoxy benzene unit benefited the generation of photocurrent and the open-circuit voltages. The polymeric metal complexes possess good thermal stability and exhibit good solubility in common organic solvents such as chloroform, THF, and toluene. The maximal power conversion efficiency of 1.21% ($J_{sc} = 2.49$ mA/cm^2, $V_{oc} = 0.695$ V, FF = 0.59) was obtained with a DSSCs based on PNi–B dye under simulated air mass 1.5 G solar irradiation.

Introduction

Recently, dye-sensitized solar cells (DSSCs) are under active investigation as a low-cost alternative to conventional inorganic silicon-based solar cells [1, 2]. These cells are very promising due to their low production cost, esthetically pleasing modules, possible mechanical flexibility, and wide application for relatively low overall cost [3]. Although there are many factors to affect the photovoltaic performance of the DSSCs, the structural, photophysical, and photoelectrochemical properties of the sensitizers are obviously crucial ones [4–8]. As a result, the pursuit of highly efficient dye stuffs has been one of the most active subjects along with the development of the DSSCs [9–12].

Ru complexes as dyes were widely used in DSSCs, due to the advantages of a wide-range absorption of visible light which is due to a metal to ligand charge transfer (MLCT) [13], suitable excited and ground state energy levels, relatively long excited state lifetime and good electrochemical stability [14]. Several Ru complexes used in DSSCs have reached over 12% power conversion efficiency under standard measurement conditions [15]. However, the rarity and high cost of the ruthenium metal may limit their development for large-scale applications [16]. Sauvage and co-workers [17] discovered that Cu(I) complexes have similar photophysical properties with Ru complexes, indicating that the iterative chemical optimization of common metal complexes sensitizers can be comparable to that of ruthenium complexes, although these initial results are not comparable with ruthenium dyes such as N719. And the "Techno-Economic" analyses of the two sensitizers clearly show that even though the efficiency of the copper complex is four times lower than that of the ruthenium sensitizer N719 [18], the cost is an order of magnitude lower [19]. Recently, Grätzel and co-workers [12] reported mesoscopic DSSCs based on donor-π-bridge-acceptor (D–π–A) zinc porphyrin dye, and the power conversion efficiency even exceeds 13%.

Compared with Ru complexes, organic dyes have attracted considerable interest in recent years because they exhibit many advantages: simple design and synthesis, tunable energy levels, sufficiently large absorption coefficient, and low fabrication costs [20]. The application of organic dyes in DSSCs has been reported recently and

J. Deng · Q. Xiu · L. Guo · L. Zhang · G. Wen · C. Zhong (✉)
Key Laboratory of Environmentally Friendly Chemistry and Applications of Ministry of Education, College of Chemistry, Xiangtan University, Xiangtan 411105, Hunan, People's Republic of China
e-mail: zhongcf798@yahoo.com.cn

D–π–A structure is the common character generally [21–25] for its intramolecular charge transfer characters (ICT) [21, 26]. So far, hundreds of *n*-type organic dyes [27], such as indoline [28], phenothiazine [29], triarylamine [30], fluorene [31], carbazole [32, 33], thiophene [3, 34] have been adopted as sensitizers for DSSCs. Among the organic dyes, thiophene-linked different functionalized group derivatives have attracted wide interest for its environmental and thermal stability, solubility, excellent conductivity, and the reversible transition [35], and the power conversion efficiency of 10.1% has been obtained based on C219 under AM 1.5 irradiation [36].

As important chelators, 8-hydroxyquinoline (8-HQ) and a functional group substituting in the 5-position of 8-HQ have been extensively used in functional metal complexes [37–39]. But the report of their application as dyes for DSSCs is rare, so there is no doubt that chemical modifications between thiophene and 8-HQ will be beneficial to the suppress charge recombination and then increase open-circuit photovoltage (V_{oc}).

In this article, we synthesized four D–π–A polymeric metal complexes as dyes for DSSCs. The polymers containing thiophene–fluorene or thiophene–phenylene [33] as the electron donor, C=C as π-conjugation linkage, Co(II) or Ni(II) metal complexes in the branched chain as the electron acceptor. The polymers are tuned by metal complexes and donor group in order to change the photophysical and electrochemical properties and thus improve the photovoltaic performance. Taking into account the solubility of polymeric metal complexes, alkoxy, or alkyl side chains are introduced in the structure. The optical, thermal, and photovoltaic properties of the resulting polymers were investigated in detail.

Experimental

Materials

All starting materials were obtained from Shanghai chemical reagent Co. Ltd. (Shanghai, China) and used without further purification. All solvents used in this work were analytical grade. *N*,*N*-Dimethylformamide (DMF) and tetrahydrofuran (THF) were dried by distillation over CaH_2. Triethylamine was purified by distillation over KOH. The other materials were common commercial grade and used as received.

Instrument and measurements

^1H NMR were performed in $CDCl_3$ and recorded on a Bruker NMR 400 spectrometer, and using TMS (0.00 ppm) as the internal reference. The FT-IR spectra were obtained on a Perkin-Elmer Spectrum One Fourier transform infrared spectrometer by incorporating samples in KBr pellets. Thermogravimetric analyses (TGA) were run on a Shimadzu TGA-7 Instrument in nitrogen atmosphere at a heating rate of 20 °C/min from 25 to 600 °C. Differential scanning calorimetry was performed on materials using a Perkin-Elmer DSC-7 thermal analyzer in nitrogen atmosphere at a heating rate of 20 °C/min from 25 to 300 °C. UV–Vis spectra were taken on a Lambda 25 spectrophotometer. Photoluminescent spectra were taken on a Perkin-Elmer LS55 luminescence spectrometer with a xenon lamp as the light source. Elemental analysis for C, H, and N was carried out using a Perkin-Elmer 2400 II instrument. Cyclic voltammetry was conducted on a CHI chi630c Electrochemical Workstation, in a 0.1 mol/L $[Bu_4N]BF_6$ DMF solution at a scan rate of 100 mV/s at room temperature. The working electrode was a glassy carbon rod, the auxiliary electrode was a Pt wire electrode, and saturated calomel electrode (SCE) was used as reference electrode. Gel permeation chromatography (GPC) analyses were performed using a Water 2414 system equipped with a set of HT3, HT4, and HT5, l-styrayel columns with THF as an eluent (1.0 mL/min) at 80 °C, calibrated by polystyrene standard.

Fabrication of DSSCs

Titania paste was prepared following a procedure: fluorine-doped SnO_2 conducting glass (FTO) were cleaned and immersed in aqueous 40 mM $TiCl_4$ solution at 70 °C for 30 min, then washed with water and ethanol, sintered at 450 °C for 30 min. The 20–30 nm particles sized TiO_2 colloid was coated onto the above FTO glass by the sliding glass rod method to obtain a TiO_2 film of 10–15 μm thickness. After drying, the TiO_2-coated FTO glass were sintered at 450 °C for 30 min, then treated with $TiCl_4$ solution and calcined at 450 °C for 30 min again. After cooling to 100 °C, the TiO_2 electrodes were soaked in 0.5 mM dye-sensitized samples PCo–F, PCo–B, PNi–F, and PNi–B in DMF solution, then kept at room temperature in the dark for 24 h. And 3-methoxypropionitrile solution containing LiI (0.5 M), I_2 (0.05 M), and 4-*tert*-butyl pyridine (TBP) (0.5 M) was used as the electrolyte. A Pt foil was used as counter electrode was clipped onto the top of the TiO_2 using as working electrode. The dye-coated semiconductor film was illuminated through a conducting glass support without a mask. And photoelectron chemical performance of the solar cell was measured using a Keithley 2602 Source meter controlled by a computer. The cell parameters were obtained under an incident light with intensity 100 mW cm^{-2}, which was generated by a 500-W Xe lamp passing through an AM 1.5 G filter with an effective area of 0.16 cm^2.

Synthesis

The synthetic routes of the monomers and polymers are shown in Scheme 1. The detailed synthesis processes are as follows.

DB8QTB–Co

A ethanol solution (10 mL) of $Co(CH_3COO)_2{\cdot}4H_2O$ (0.124 g, 0.5 mmol) was dropped to a mixed THF solution (20 mL) of 2,5-dibromo-3-[2-(8-hydroxyquinoline)-vinyl]-thiophene (DB8QTH) [40] (0.205 g, 0.5 mmol) and 2,2′-dipyridyl (0.078 g, 0.5 mmol). The reaction mixture was neutralized carefully with 1 M aq. sodium hydroxide until neutral to slightly acidic pH and was refluxed overnight, then recrystallized from ethanol. Filtered, washed with ethanol and water repeatedly, the yellow precipitate was collected. Yield: 0.22 g, 64%. FT-IR (KBr, cm^{-1}): 3064, 3019 (aromatic and vinylic C–H), 1561 (C=N), 1512 (C=C), 1012 (C–O–M), 502 (N–M). Anal. Calcd for $[C_{27}H_{19}SO_3N_3Br_2Co]$: C, 47.39; H, 2.80; N, 6.14; S, 4.69; Found: C, 47.55; H, 2.83; N, 6.32; S, 4.58%.

DB8QTB–Ni

It was prepared following the same procedures as for DB8QTB–Co affords a yellow solid. Yield: 55%. FT-IR (KBr, cm^{-1}): 3132, 2942 (aromatic and vinylic C–H), 1576 (C=N), 1513 (C=C), 1046 (C–O–M), 501 (N–M). Anal. Calcd For $[C_{25}H_{16}SO_4N_4Br_2Ni]$: C, 43.71; H, 2.35; N, 8.16; S, 4.67; Found: C, 43.87; H, 2.42; N, 8.13; S, 4.82%.

1,4-Divinyl-2-methoxyl-5-octyloxy benzene

Under nitrogen atmosphere, a mixture of formaldehyde aqueous (18 mL) and 1,4-bis(bromomethyl)-2-methoxyl-5-octyloxybenzenetriphenyl-phosphonium salt (synthesized according to the literature [41]) (4.257 g, 4.5 mmol) in dichloromethane (60 mL) was stirred at 0 °C, then an aqueous solution of NaOH (20 wt%, 39 mL) was added by dropwise in 1 h. After reaction mixture was stirred for 24 h, the aqueous layer of resulting solution was extracted with dichloromethane three times. The combined organic layer was washed with water and dried with anhydrous $MgSO_4$. Subsequently, the solvent was removed by rotary evaporation. The crude product was further purified by column chromatography (eluent:*n*-hexane/dichloromethane = 7:2) to afford light yellow liquid. Yield: 0.648 g, 50%. ^1H NMR (400 MHz, $CDCl_3$, δ, ppm): 7.10–7.03 (m, 1H), 7.01 (s, 2H), 5.78–5.71 (d, 2H), 5.29–5.26 (d, 2H), 3.99–3.98 (t, 2H), 3.85 (s, 3H), 1.85–1.81 (m, 12H), 0.91–0.81 (t, 3H).

2,7-Divinyl-9,9-dioctylfluorene

A solution of 2,7-bis(bromomethyl)-9,9-dioctylfluorene-triphenyl-phosphonium salt (synthesized according to the

Scheme 1 Synthesis of the comonomers and copolymers

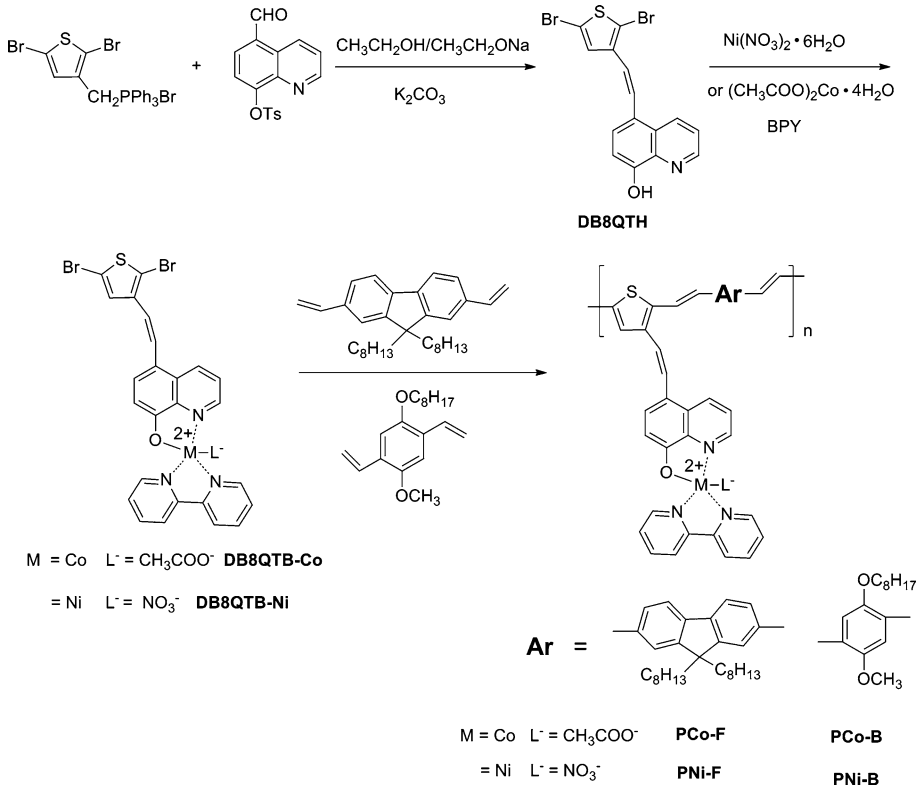

literature [41]) (0.45 g, 0.445 mmol) and 37% formaldehyde solution (0.3 g, 3.56 mmol) in 10 mL of chloroform was added dropwise with a solution of potassium *tert*-butoxide (0.45 g, 4 mmol) dissolved in 10 mL of EtOH. After stirring for 5 h, the solution was poured into an excess of ice water. The organic layer was successively washed with water twice, dried with anhydrous $MgSO_4$ and filtered off, followed with solvent removal under reduced pressure. The crude product was further purified by column chromatography using *n*-hexane as an eluent to afford colorless liquid. (Yield: 0.177 g, 90%). ^{1}H NMR (400 MHz, $CDCl_3$, δ, ppm): 7.64–7.62 (d, 2H), 7.37–7.41 (m, 4H), 6.78–6.85 (m, 2H), 5.79–5.83 (d, 2H), 5.26–5.28 (d, 2H), 1.95–1.99 (m, 4H),1.06–1.32 (m, 24H). 0.81–0.96 (t, 6H).

Polymeric metal complex PCo–F

The polymeric metal complex PCo–F was synthesized by the Heck coupling method, according to the literature [42]. A flask was charged with a mixture of DB8QTB–Co (0.2155 g, 0.315 mmol), 2,7-divinyl-9,9-dioctylfluorene (0.0602 g, 0.315 mmol), $Pd(OAc)_2$ (0.0029 g, 0.013 mmol), tri-*o*-tolylphosphine (0.0220 g, 0.072 mmol), DMF (8 mL) and triethylamine (3 mL). The flask was degassed and purged with N_2. The mixture was heated at 90 °C for 36 h under N_2. Then, it was filtered and the filtrate was poured into methanol. The purple precipitate was filtered and washed with methanol. The crude product was purified by dissolving in THF and precipitating into methanol to afford a red solid. (Yield: 0.146 g, 60%). FT-IR (KBr, cm^{-1}): 2921, 2849, 1632, 1598, 1463, 1441, 1307,1258, 1206, 1171, 1093, 958, 902, 834, 756, 509. Anal. Calcd for [$C_{60}H_{63}SO_3N_3Co$]: C, 74.67; H, 6.58; N, 4.35; S, 3.32; Found: C, 74.84; H, 6.72; N, 4.46; S, 3.41%.

Polymeric metal complex PCo–B

With the similar synthetic method as PCo–F afford a red solid. Yield: 53%. FT-IR (KBr, cm^{-1}): 3056, 2922, 2852 (aromatic and vinylic C–H), 1588 (C=N), 1513 (C=C), 943 (C–O–M). Anal. Calcd for [$C_{46}H_{43}SO_5N_3Co$]: C, 68.31; H, 5.36; N,5.20; S, 3.96; Found: C, 68.48; H, 5.58; N, 5.13; 3.81%.

Polymeric metal complex PNi–F

With the similar synthetic method as PCo–F afford a yellow solid. Yield: 56%. FT-IR (KBr, cm^{-1}): 3061, 2930, 2849 (aromatic and vinylic C–H), 1606 (C=N), 1466 (C=C), 926 (C–O–M). Anal. Calcd for [$C_{58}H_{60}SO_4N_4Ni$]: C, 71.97; H, 6.25; N, 5.79; S, 3.31; Found: C, 72.15; H, 6.43; N, 5.91; S, 3.26%.

Polymeric metal complex PNi–B

With the similar synthetic method as PCo–F afford a red solid. Yield: 64%. FT-IR (KBr, cm^{-1}): 3032, 2930, 2849 (aromatic and vinylic C–H), 1597 (C=N), 1448 (C=C), 902 (C–O–M). Anal. Calcd for [$C_{44}H_{40}SO_6N_4Ni$]: C, 65.12; H, 4.97; N, 6.90; S, 3.95; Found: C, 65.24; H, 5.21; N, 5.79; S, 3.90%.

Results and discussion

Synthesis and characterization

Scheme 1 illustrates the synthetic routes of the metal complexes DB8QTH-M and the four branched chain polymeric metal complexes (PCo–F, PCo–B, PNi–F, and PNi–B) which were synthesized by the Heck coupling [43]. In particular, 1,4-divinyl-2-methoxyl-5-octyloxy benzene or 2,7-divinyl-9,9-dioctylfluorene reacted with DB8QTB–M in a molar ratio of 1:1 to afford the alternating polymeric metal complexes PCo–F, PCo–B, PNi–F, and PNi–B, respectively. These reactions took place in DMF solution utilizing triethylamine as an acid acceptor. The products were purified by dissolving in THF and precipitating into methanol.

Figures 1 and 2 depict the IR spectra of metal complexes (DB8QTB–Co, DB8QTB–Ni) and polymeric metal complexes (PCo–F, PCo–B, PNi–F, and PNi–B), respectively. The present of broad absorption band in the region 3,450–3,320 cm^{-1} is probably due to the existence of lattice and/or coordinated water in the molecule, and make it difficult to see the bands due to the O–H stretching vibrations, which would appear in this region. The metal

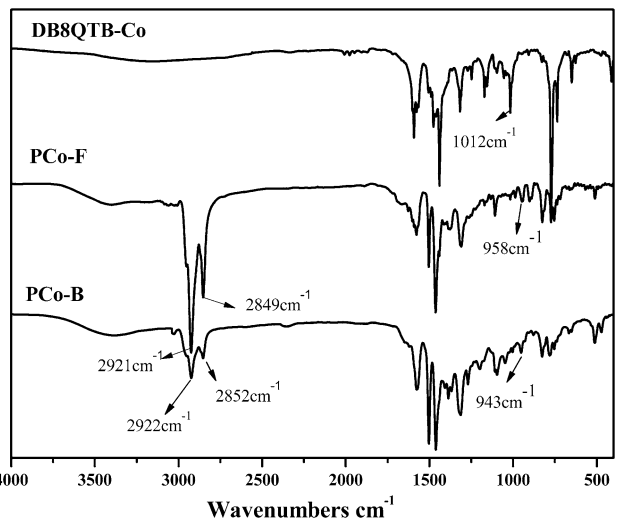

Fig. 1 FT-IR spectra of polymers PCo–F and PCo–B

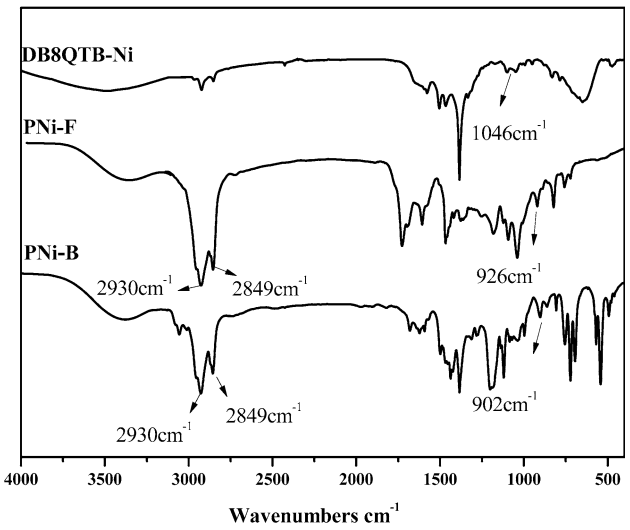

Fig. 2 FT-IR spectra of polymers PNi–F and PNi–B

complexes and polymeric metal complexes have similar bands, but the sharp absorption bands at 958, 943, 926, and 902 cm^{-1} for the PCo–F, PCo–B, PNi–F, and PNi–B, respectively, are shown redshift compared with metal complexes, which should be associated with C–O vibrations at the C–O–M site [41]. Four polymeric metal complexes have similar bands at 2,922 and 2,847 cm^{-1}, which are associated with the CH_2 asymmetric and symmetric stretching vibration, respectively. This suggests that alkoxy benzene or octyl fluorene has been successfully embedded in the molecular chain. It can prove that target products have been successfully synthesized taken together with the data of the average molecular weight and elemental analysis.

The GPC studies show that four dyes (PCo–F, PCo–B, PNi–F, and PNi–B) have number average molecular weight at 14.6, 16.5, 10.6, and 12.7 kg/mol with a polydispersity index (PDI) of 1.54–1.78 (Table 1). The repeating units on average of PCo–F, PCo–B, PNi–F, and PNi–B are 15, 20, 11, and 15, respectively. As expected, all the dyes show good solubility and can be soluble in common organic solvents, such as, THF, toluene, DMSO, and DMF.

UV–Vis absorption and fluorescence spectra

The UV–Vis absorption spectra of the ligand and the polymeric metal complexes in THF solution are shown in Fig. 3, and the corresponding optical data are summarized in Table 1. The ligand DB8QTH shows a UV–Vis normalized absorption peak located at 360 nm, corresponding to the π–π^* electron transitions of the conjugated molecules, which was observed in the ICT between the electron acceptor 8-hydroxyline unit and the electron donating thiophene moiety [40]. In comparison with ligand DB8QTH, λ_{max} of PCo–F, PCo–B, PNi–F, and PNi–B distributed in 326–353 nm, they show blue-shifted 7–36 nm because of electron withdrawing Co(II) or Ni(II) ions in the branched chain. There are longer absorption tail extending beyond 600 nm for PCo–F–PNi–B, which can be assigned to the MLCT transition and the overlapped with that of the π–π^* intraligand transition of bpy [44]. This is the further evidence of the incorporation of the Co(II) or Ni(II) complex into the polymers. The peaks around 462–492 of PNi–F and PCo–F are higher that that of PCo–B and PNi–B, and this phenomena might be due to the fact that octyl fluorene unit has stronger electron donating ability than that of alkoxy benzene unit.

Table 1 Molecular weights, thermal and optical properties of copolymers

Polymer	PCo–F	PCo–B	PNi–F	PNi–B
$\overline{M}_n$ ($\times 10^3$)	14.6	16.5	10.6	12.7
$\overline{M}_w$ ($\times 10^3$)	22.5	26.5	17.6	22.6
PDI	1.54	1.61	1.66	1.78
T_g (°C)	161	123	157	131
T_d (°C)	304	322	289	300
$\lambda_{a,max}$, $\lambda_{a,onset}$	329; 483	353; 492	353; 468	326,380; 462
$\lambda_{p,max}$	412	452	361	469
HOMO (eV)	−5.707	−5.735	−5.783	−5.846
LUMO (eV)	−3.538	−3.469	−3.566	−3.553
E_g^{EC} (eV)	2.169	2.266	2.217	2.293

$\overline{M}_n$, $\overline{M}_w$, and PDI of the polymers were determined by GPC using polystyrene standards in THF

Glass transition temperature (T_g) measured from DSC traces of the polymeric metal complexes

The temperature of degradation (T_d) corresponding to a 5% weight loss determined by TGA at a heating rate of 10 °C/min

$\lambda_{a,max}$, $\lambda_{a,onset}$ maxima and onset absorption from the UV–Vis spectra in DMF solution, $\lambda_{p,max}$ PL maxima in DMF solution, E_g^{EC} electrochemical band gap determined from cyclic voltammetry

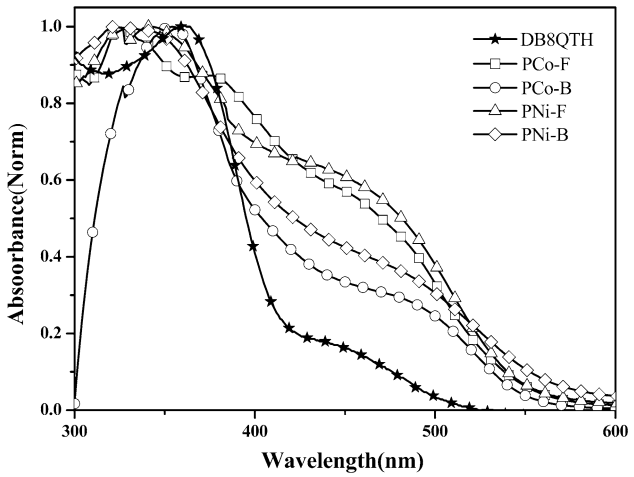

Fig. 3 UV–Vis absorption spectra of PCo–F, PCo–B, PNi–F, and PNi–B in the THF solution (10^{-5} M)

The photoluminescence (PL) emission spectra of the four polymeric metal complexes in THF solution are shown in Fig. 4. The excitation wavelengths were set to the absorption maxima from the UV–Vis absorption spectra. In comparison with PCo–F (412 nm) and PNi–F (361 nm), the maximum emissions of PCo–B (452 nm) and PNi–B (469 nm) are obviously red-shifted due to the octyl fluorene unit in the molecular chain. It indicates that donor unit plays a key role in fluorescent emission of the dyes. The maximum emission of PNi–B is red-shifted 17 nm relative to PCo–B because d^7 Co(II) has few electron than d^8 Ni(II) which can accept electron from ligand easily. The maximum emission of PCo–F is red-shifted 51 nm relative to PNi–F, and this can be attribute to PCo–F has longer conjugation lengths, which leads to educe non-radiative decay of the intraligand (π–π^* transition) excited state and decrease the energy gap between the π and π^* molecular orbits of the ligand [45]. The corresponding optical data of the polymeric metal complexes are also summarized in Table 1.

Thermal stability

The thermal properties of the polymeric metal complexes were investigated by TGA and differential scanning calorimetric (DSC) analysis, and the corresponding data are also reported in Table 1. The TGA (Fig. 5) results reveal that PCo–F, PCo–B, PNi–F, and PNi–B possess good thermally stability with 5% weight loss at temperatures (T_d) of 304, 322, 289, and 300 °C in nitrogen, respectively. It is seen that PCo–F, PCo–B, PNi–F, and PNi–B have glass transition temperature (T_g) ranged from 123 to 161 °C and followed the order PCo–F > PNi–F > PNi–B > PNi–B. This suggests that fluorenevinylene unit embedded in the polymer backbones renders higher rigidity compared with the phenylenevinylene units. The T_g of the four polymers can be comparable to poly(9,9-di-*n*-octyl-fluorene-2,7-vinylene) (T_g = 173 °C) [46]. High glass transitions temperature shows that these polymeric metal complexes will be a kind of valuable material for solar cell material.

Electrochemical properties

To estimate the highest occupied molecular orbital (HOMO) and lowest unoccupied molecular orbital (LUMO) energy levels of the polymers, which is an important property for organic materials used in solar cells, cyclic voltammetry method was employed in DMF solution containing $[Bu_4N]BF_6$ as supporting electrolyte and SCE as reference electrode at a scan rate of 100 mV/s, and all the electrochemical properties of the polymers are listed

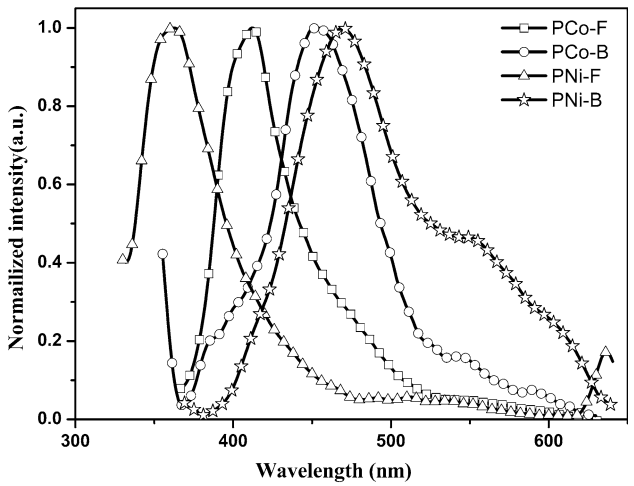

Fig. 4 PL spectra of PCo–F, PCo–B, PNi–F, and PNi–B in the THF solution (10^{-5} M)

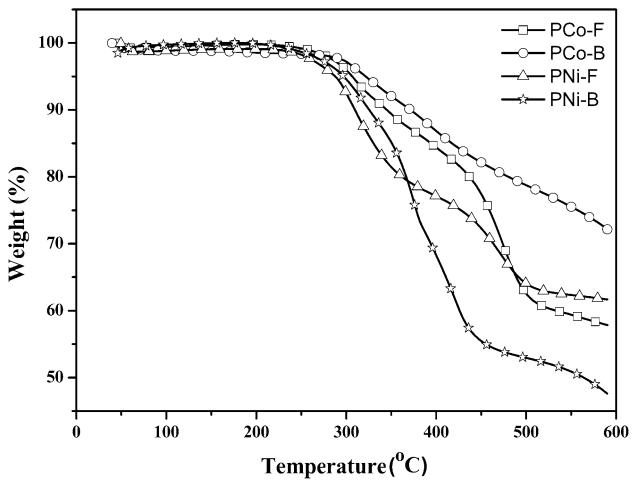

Fig. 5 TGA plots of PCo–F, PCo–B, PNi–F, and PNi–B with a heating rate of 20 °C/min under nitrogen atmosphere

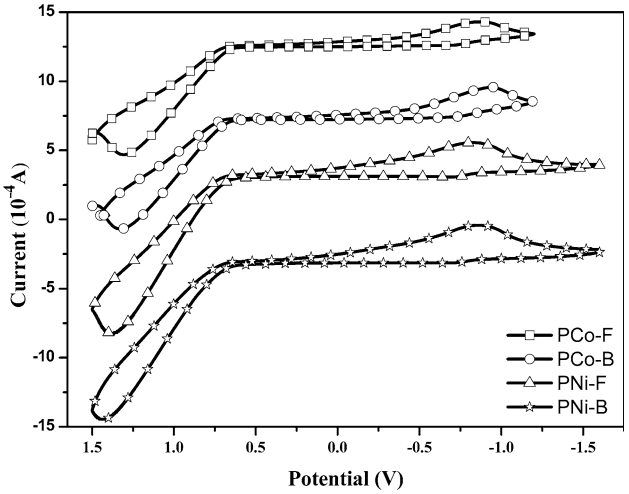

Fig. 6 Cyclic voltammograms of PCo–F, PCo–B, PNi–F, and PNi–B measured in DMF solution containing $[Bu_4N]BF_6$ as supporting electrolyte at a scan rate of 100 mV/s

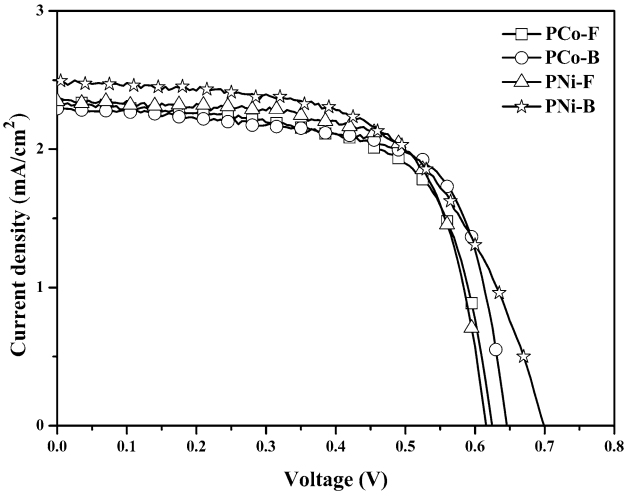

Fig. 7 *J–V* curves of DSSCs based on PCo–F, PCo–B, PNi–F, and PNi–B in DMF solution

in Table 1. As observed from the cyclic voltammograms in Fig. 6, all polymers exhibited irreversibility processes. The HOMO and LUMO are measured by electrochemical cyclic voltammetry, where SCE electrode was used as the reference electrode. The correlation can be expressed as the equation [47, 48]:

$$\text{HOMO} = -\text{e}(E_{\text{ox}} + 4.40)\ (\text{eV})$$

$$\text{LUMO} = -\text{e}(E_{\text{red}} + 4.40)\ (\text{eV})$$

$$E_{\text{g}} = \text{HOMO} - \text{LUMO}$$

The HOMO energy values of PCo–F, PCo–B, PNi–F, and PNi–B were estimated to be −5.707, −5.735,−5.783, and −5.846 eV versus SCE, respectively, which are 0.877–1.016 eV lower than the standard potential of the I_3/I^- redox couple (−4.83 eV vs vacuum). This indicates that sufficient driving forces for the regeneration of the oxidized dyes are available. The LUMO energy levels [PCo–F: −3.538 eV; PCo–B: −3.469 eV; PNi–F: −3.566 eV; PNi–B: −3.553 eV] are sufficiently higher than the conduction band edge of TiO_2 (−4.0 eV) [49], which indicates that effective electron transfer from the excited dye to the TiO_2 is ensured. The energy band gap (E_g) of the polymers follows the order of PCo–F (2.169 eV) < PNi–F (2.217 eV) < PCo–B (2.266 eV) < PNi–B (2.293 eV), which might be in that octyl fluorene unit has stronger electron donating ability than that of alkoxy benzene unit and then the energy gap is decreased. PCo–F has the minimum E_g relative to other three polymers which can be attribute to PCo–F has the longest conjugation lengths.

Photovoltaic properties

Figure 7 shows the irradiation source for the photocurrent density–voltage *J*–V) measurement of the DSSCs devices based on the four polymeric metal complexes (PCo–F, PCo–B, PNi–F, and PNi–B). The corresponding open-circuit voltage (V_{oc}), short-circuit current density (J_{sc}), fill factor (FF), and power conversion efficiency (η) are summarized in Table 2. It can be seen that the J_{sc} follows the order of PCo–B (2.294 mA/cm^2) < PCo–F (2.324 mA/cm^2) < PNi–F (2.346 mA/cm^2) < PNi–B (2.490 mA/cm^2). The V_{oc} values of PCo–F, PCo–B, PNi–F, and PNi–B fill 0.625, 0.645, 0.615, and 0.695 V, respectively, and the corresponding FF values are 0.66, 0.683, 0.693, and 0.59.

The η based on PNi–B (1.21%) is higher than that of the device based on PCo–F (0.96%), PCo–B (1.01%), and PNi–F (1.00%), which result from the highest V_{oc} and J_{sc} of PNi–B than other three dyes. This could be because the d^8 Ni(II) complex possesses higher kinetic stability than d^7 Co(II) complex, and alkoxy benzene unit has more conducive to the generation of photocurrent and the open-circuit voltages than that of octyl fluorene unit. However, all of the J_{sc} are low which is ascribed to the low charge separation, transportation efficiency, and the weak adsorption onto the surface of TiO_2 [15]. These initial results are not comparable with state of the ruthenium dyes such as N3, and further work on optimizing the device performance is under investigation.

Table 2 The data of photovoltaic performances of DSSCs

Polymer	Solvent	J_{sc} (mA/cm^2)	V_{oc} (V)	FF	η (%)
PCo–F	DMF	2.324	0.625	0.66	0.96
PCo–B	DMF	2.294	0.645	0.683	1.01
PNi–F	DMF	2.346	0.615	0.693	1.00
PNi–B	DMF	2.490	0.695	0.59	1.21

Conclusions

In summary, we demonstrate the synthesis and characterization of four novel D–π–A polymeric metal complexes PCo–F, PCo–B, PNi–F, and PNi–B with Co(II) or Ni(II) complexes in the branched chain. The target products have showed good solubility, outstanding stabilities and good open-circuit voltages but moderate power conversion. The η of PCo–F, PCo–B, PNi–F, and PNi–B are 0.96, 1.01, 1.00, and 1.21%, respectively, indicating the importance of their further investigation in DSSCs.

There are still many challenges to obtain outstanding η, the weak adsorption affinities on the TiO_2, high energy band gap, inefficient light absorption and ICT are the main reasons that we cannot obtain outstanding η [50]. So we managed to introduce one or two anchoring groups such as –CN, –COOH, $–H_2PO_3$, or $–SO_3H$ to the structure, and use metal ion which has more electrons and donor unit with strong electron donating ability to tune the energy level. Besides, the further structural optimization for efficient charge separation and transportation is expected to improve the performance of DSSCs. Our works toward these directions are underway.

References

1. O'Regan B, Grätzel M (1991) Nature 353:737
2. Grätzel M (2005) Inorg Chem 44:6841
3. Fang Z, Eshbaugh AA, Schanze KS (2011) J Am Chem Soc 133:3063
4. Nazeeruddin MK, Péchy P, Renouard T, Zakeeruddin SM, Humphry-Baker R, Comte P, Liska P, Cevey L, Costa E, Shklover V, Spiccia L, Deacon GB, Bignozzi CA, Grätzel M (2001) J Am Chem Soc 123:1613
5. Grätzel M (2004) J Photochem Photobiol A Chem 164:3
6. Wang P, Zakeeruddin SM, Moser JE, Nazeeruddin MK, Sekiguchi T, Grätzel M (2003) Nat Mater 2:402
7. Chen CY, Wu SJ, Wu CG, Chen JG, Ho KC (2006) Angew Chem Int Ed 45:5822
8. Bessho T, Yoneda E, Yum JH, Guglielmi M, Tavernelli I, Imai H, Rothlisberger U, Nazeeruddin MK, Grätzel M (2009) J Am Chem Soc 131:5930
9. Hwang S, Lee JH, Park C, Lee H, Kim C, Park C, Lee MH, Lee W, Park J, Kim K, Park NG, Kim C (2007) Chem Commun 4887
10. Lan Z, Wu J, Lin J, Huang M (2010) J Mater Sci: Mater Electron 21:1000
11. Macwan DP, Dave PN, Chaturvedi S (2011) J Mater Sci 46:3669. doi:10.1007/s10853-011-5378-y
12. Yella A, Lee HW, Tsao HN, Yi C, Chandiran AK, Nazeeruddin MK, Diau EWG, Yeh CY, Zakeeruddin SM, Grätzel M (2011) Science 334:629
13. Chou CC, Wu KL, Chi Y, Hu WP, Yu SJ, Lee GH, Lin CL, Chou PT (2011) Angew Chem Int Ed 50:2054
14. Wang YM (2009) Sol Energy Mater Sol Cells 93:1167
15. Hagfeldt A, Boschloo G, Sun LC, Kloo L, Pettersson H (2010) Chem Rev 110:6595
16. Chen RK, Yang XC, Tian HN, Wang XN, Hagfeldt A, Sun LC (2007) Chem Mater 19:4007
17. Alonso-Vante N, Nierengarten JF, Sauvage JP (1994) J Chem Soc Dalton Trans 1649
18. Nazeeruddin MK, Splivallo R, Liska P, Comte P, Grätzel M (2003) Chem Commun 1456
19. Bessho T, Constable EC, Grätzel M, Redondo RA, Housecroft CE, Kylberg W, Nazeeruddin MK, Neuburger M, Schaffner S (2008) Chem Commun 3717
20. Zhang W, Fang Z, Su M, Saeys M, Liu B (2009) Macromol Rapid Commun 30:1533
21. Hagberg DP, Yum JH, Lee H, De Angelis F, Marinado T, Karlsson KM, Humphry-Baker R, Sun LC, Hagfeldt A, Grätzel M, Nazeeruddin MK (2008) J Am Chem Soc 130:6259
22. Cai N, Moon SJ, Cevey-Ha L, Moehl T, Humphry-Baker R, Wang P, Zakeeruddin SM, Grätzel M (2011) Nano Lett 11:1452
23. Mai CL, Huang WK, Lu HP, Lee CW, Chiu CL, Liang YR, Eric WGD, Yeh CY (2010) Chem Commun 809
24. Li W, Wu Y, Li X, Xie Y, Zhu W (2011) Energy Env Sci 4:1830
25. Marszalek M, Nagane S, Ichake A, Baker RH, Paul V, Zakeeruddin SM, Grätzel M (2012) J Mater Chem. doi:10.1039/c1jm14024h
26. Horiuchi T, Miura H, Sumioka K, Uchida S (2004) J Am Chem Soc 126:12218
27. Qin P, Wiberg J, Gibson EA, Linder M, Li L, Brinck T, Hagfeldt A, Albinsson B, Sun L (2010) J Phys Chem C 114:4738
28. Ito S, Miura H, Uchida S, Takata M, Sumioka K, Liska P, Comte P, Péchy P, Grätzel M (2008) Chem Commun 5194
29. Cao D, Peng J, Hong Y, Fang X, Wang L, Meier H (2011) Org Lett 13:1610
30. Chen BS, Chen DY, Chen CL, Hsu CW, Hsu HC, Wu KL, Liu SH, Chou PT, Chi Y (2011) J Mater Chem 21:1937
31. Grisorio R, Mastrorilli P, Suranna GP, Cosma P, Marco LD, Manca M, Gigli G (2011) J Polym Sci A 49:842
32. Ooyama Y, Inoue S, Nagano T, Kushimoto K, Ohshita J, Imae I, Komaguchi K, Harima Y (2011) Angew Chem Int Ed 50:7429
33. Zhang W, Tao F, Meng K, Wang Z, Xi L, Li Y, Jiang Q (2011) J Mater Sci 46:5363. doi:10.1007/s10853-011-5474-z
34. Yang YS, Kim HD, Ryu JH, Kim KK, Park SS, Ahn KS (2011) Synth Met 161:850
35. Lee SM, Lee SB, Kim KH, Cho SE, Kim YK, Park HW, Lee JK, Kim MR (2011) Sol Energy Mater Sol Cells 95:306
36. Zeng WD, Cao YM, Bai Y, Wang YH, Shi YS, Zhang M, Wang FF, Pan CY, Wang P (2010) Chem Mater 22:1915
37. Xie J, Ning Z, Tian H (2005) Tetrahedron Lett 46:8559
38. Saylam A, Seferoglu Z, Ertan N (2008) Dyes Pigm 76:470
39. Luo JX, Yang CL, Liang LY, Lu MG (2011) J Polym Res 18:1197
40. Xiao LF, Liu Y, Xiu Q, Zhang LR, Guo LH, Zhang HL, Zhong CF (2010) Tetrahedron 66:2835
41. Xiao LF, Liu Y, Xiu Q, Zhang LR, Guo LH, Zhang HL, Zhong CF (2010) J Polym Sci A 48:1943
42. Tsai LR, Chen Y (2008) J Polym Sci A 46:70
43. Ziegler CB, Heck RF (1978) J Org Chem 43:2941
44. Yuan S, Jaramillo R, Rosenbaum TF, Yu L (2006) Macromolecules 39:8652
45. Zhong C, Guo R, Wu Q, Zhang H (2007) React Funct Polym 67:408
46. Jin SH, Park HJ, Kim JY, Lee K, Lee SP, Moon DK, Lee HJ, Gal YS (2002) Macromolecules 35:7532
47. Li XZ, Zeng WJ, Zhang Y, Hou Q, Yang W, Cao Y (2005) Eur Polym J 41:2923
48. Agrawal AK, Jenekhe SA (1996) Chem Mater 8:579
49. Zhang G, Baba H, Cheng Y, Shi D, Lv X, Yu Q, Wang P (2009) Chem Commun 2198
50. Wang ZS, Li FY, Huang CH (2001) J Phys Chem B 105:9210